Efficiency Analysis of Various Batteries with Real-time Data on a Hybrid Electric Vehicle

Yunus Emre Ekici[1*], İsmail Can Dikmen[1], Mustafa Nurmuhammed[1] and Teoman Karadağ[2]

0000-0001-7791-0473, 0000-0002-7747-7777, 0000-0002-5957-3255, 0000-0002-7682-7771

[1]Department of Electric Vehicle Technologies Inonu University OSB Vocational School, Malatya, Turkey
[2]Department of Electric Electronic Engineering Inonu University, Malatya, Turkey,

Abstract

Battery selection remains an up-to-date engineering problem for hybrid and electric vehicle manufacturers. Type of battery and its capacity will depend on the trip and vehicle parameters. An electric vehicle produced with the ideal battery type will undoubtedly be preferred by customers. Data collected from black boxes of trolleybuses operated by Malatya Metropolitan Municipality were used in this study. The real road and driver characteristics were included in the study with the experimentally obtained data. These data are the accelerator pedal data obtained from vehicles driven by different drivers in regular and congested traffic hours. In this study, four different battery chemistries were run separately on a hybrid vehicle model and analyzed. Chosen battery chemistries are the most commonly used by manufacturers. These are Lead Acid, Nickel Cadmium, Nickel Metal Hydride and Lithium Iron Phosphate batteries. The results of the study are presented in detail comparatively. Among the battery chemistries, Lithium iron phosphate is observed to be the most ideal battery type for hybrid electric vehicles.

Keywords: Electric vehicles, Hybrid vehicles, Batteries, Battery management system

1. Introduction

In today's world, besides the decrease in energy resources, the environmental problems caused by fossil fuels and the increase of environmental sensitivity in individuals reinforce the importance of renewable energy resources. For this reason, studies on renewable energy sources are increasing rapidly. One of the focal points of these studies is sustainable transportation, which is vehicles powered by renewable energy (1). Leaving the internal combustion engine technology that has dominated the automotive industry for years and completely transitioning to electric vehicle technology, it is seen as a risk factor for vehicle manufacturers (2). In addition, the lack of financial and political support provided by governments is another factor that reduces consumers' interest in electric vehicles (3). Vehicle manufacturers also face a dilemma in the face of these adverse situations (4,5).

Technology behind electric vehicles dates back to mid-19th century (6). However, since the energy storage problem could not be overcome, it had to be supported by internal combustion engines (7). This was a driving reason for the development of hybrid electric vehicles. Therefore, it can be said that hybrid vehicles are a transition between fossil fuel vehicles and electric vehicles (8). The main problem of automotive manufacturers in the development process of hybrid and electric vehicles has always been related to batteries. At this point, the optimal selection of batteries' cost, safety, energy storage capacity and lifespan are critical parameters not only in the vehicle manufacturing process but also in every stage of life cycle. Choosing the right battery is of great importance for manufacturers working on the concept of hybrid electric vehicles. Currently, three types of battery chemistry are preferred in electric vehicle technologies and are widely used for automotive applications. These types are; lead acid (Pb-Acid), nickel metal hydride (Ni-Mh) and lithium based batteries. Lead acid batteries, which are widely used in automobiles, consist of six cells connected in series (9). In such batteries, the anode of each cell is made of lead. The cathode part is made of lead dioxide placed on a metal plate (10). The cathode and anode are immersed in a sulfuric acid solution that acts as an electrolyte (11). Lead acid batteries are widely preferred by manufacturers as they are used in systems such as lighting, starting and ignition due to their low cost. Besides, they are also used in vehicles such as golf carts and wheelchairs as the main power source (12). Nickel metal hydride batteries are one of the frequently used battery types for electric vehicles. For

example, nickel metal hydride batteries were used in the General Motors EV1 electric car, which was the first mass production electric vehicle (13). In recent decades, various lithium-based battery technologies have been studied and developed for their ability to be used in battery electric vehicles and hybrid electric vehicles (14). Some of the lithium-based batteries are Lithium Iron Phosphate (LFP), Lithium Titanate Oxide (LTO) and Lithium Sulfur Dioxide batteries (15).

Lithium iron phosphate (LiFePO4 - LFP) batteries play a dominant role in the electric vehicle industry because they are less affected by changes in ambient temperature, they can work more efficiently at high temperatures, charge relatively faster, and most importantly, they are safer on the basis of these features. For applications requiring high power, such as with an electric vehicle, the preferred LFP battery cells have an average nominal cell voltage of 3.3 Volts (16). This kind of batteries have a relatively slow capacity fade compared to other lithium-based batteries and have a longer shelf life. LFP batteries are gaining popularity day by day among automobile manufacturers and the R&D community as they can maintain their nominal voltage in the 10% - 90% state-of-charge range (17–19).

The general parameters of these three types of batteries mentioned above are presented in Table 1. As can be seen that lithium iron phosphate (LFP) batteries are the most suitable battery type for use in electric vehicles with their high energy density, long working life and high reliability (3,20,21).

Table 1. General technical specifications of batteries with different chemistry used in electric vehicles

Parameters	Lead Acid	Nickel Metal Hydride	Lithium Ion	Ni Cd
Nominal Voltage (V)	2	3.2	3.6-3.7	1.2
Charge Voltage (V)	16	3.7	3.7	1.4
Life (Cycles)	2000	1500	3000	2000
Operating Temperature (C)	60	100	80	50
Safety	Low	Medium	Good	Good
Energy Density (Wh/kg)	40	70	150	60

The fact that battery types have different voltage and current levels allows each battery pack to operate in different ranges. In this study, by modeling a hybrid electric vehicle and using real operation data, the accelerator pedal signals of different days and hours are examined by applying them on two different scenarios (22–25). These data have been processed based on specified driving scenarios and have provided a real driving experience with different battery types for the hybrid vehicle. In our previous studies (26,27) tests were carried out on four different battery chemistries with different driving scenarios and the data obtained were presented in tables and figures (28).
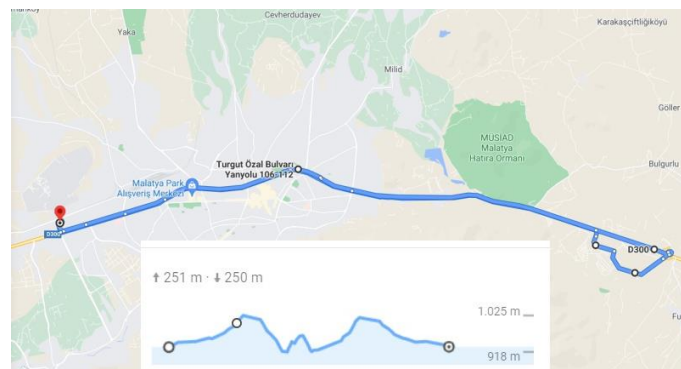

Fig. 1. Malatya city trolleybus route and elevation profile

In this study, more realistic data was obtained with the accelerator pedal signals received from a fully electric trolleybus vehicle (29,30). These vehicles provide public transportation services in Malatya city between Inonu University on the east side and the intercity bus terminal on the west side. This route is 38.2 km long and is shown in Figure 1.

The accelerator pedal signals used were taken from the black boxes integrated into the communication line. The aim here is to integrate the hybrid electric vehicle modeled by taking the real accelerator pedal signals of different drivers, and enable the hybrid electric vehicle to operate on the same route (31). When a hybrid vehicle is in operation, the electric motor must be activated and deactivated according to the power required. When the electric motor is activated, the batteries will begin to discharge and when the electric motor is deactivated, the batteries will begin to charge (31). During this application, a parameter was needed to define the transition of the vehicle from the internal combustion engine to the electric engine (9). For this reason, hybrid mode has been defined. The charge and discharge characteristics of four different types of batteries have been investigated on this model.

2. Material and Methods

2.1 Vehicle Dynamic Model

The motion of an object is the result of the forces acting on that object. From such a simple perspective, the motion of an electric vehicle, despite its complexity, can be calculated according to the resultant of the forces acting on it. This is called the mathematical model of the vehicle. Therefore, the movement of the vehicle can be modeled by examining the forces acting on the vehicle separately. The forces acting on the vehicle are as in Figure 2.
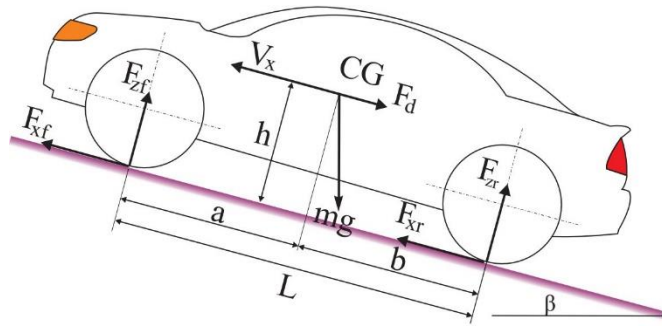
Fig. 2.   Forces acting on the vehicle (32)

These forces can be calculated with the help of the following equations.

$$mV̇_x = F_x - F_d - mg \sin \beta \qquad (1)$$

$$F_x = n(F_{xf} + F_{xr}) \qquad (2)$$

$$F_d = \frac{1}{2} C_d \rho A (V_x + V_\omega)^2 \qquad (3)$$

$$F_{zf} = \frac{-h(F_d + mg \sin \beta + mV̇_x) + bmg \cos \beta}{n(a+b)} \qquad (4)$$

$$F_{zr} = \frac{h(F_d + mg \sin \beta + mV̇_x) + amg \cos \beta}{n(a+b)} \qquad (5)$$

Here;
CG: Center of gravity
h: Height of the center of gravity
g: Gravitational acceleration
m: Total mass of the vehicle
β: Angle of inclination
a, b: The distance of the projection of the center of gravity to the axle plane to the front and rear axle
V_x: Vehicle speed
V_ω: Wind speed
n: Number of wheels on each axle
F_{xf}, F_{xr}: Longitudinal forces at the point of contact of the front and rear wheels with the ground
F_{zf}, F_{zr}: Normal forces at the point of contact of the front and rear wheels with the ground
A: Effective front area of the vehicle
C_d: Aerodynamic drag coefficient
ρ: Air density
F_d: Aerodynamic drag force

The state of the car can be simulated instantaneously with the functions created while the vehicle is in motion. At this point, the dynamic model of the vehicle alone is not sufficient for a realistic simulation. In addition, parts such as mechanical connection assembly, engine, and electrical systems should be included in the model.

2.1 Mechanical Coupler Model

In parallel hybrid and serial parallel hybrid vehicles, the internal combustion engine and electric motor provide the traction required for the vehicle together or separately. The power from both motors is brought together by a mechanical link which generally has two types: torque connection and speed connection [16]. In the torque connection, the torques obtained from the internal combustion engine and the electric motor are combined and transmitted to the axle. In the speed connection, the speeds of the internal combustion engine and the electric motor are added together with their torques. In this case, they cannot be controlled independently. In a no-loss (ideal) torque connection, the input power and output power are equal. In this case;

$$T_3 \omega_3 = T_1 \omega_1 + T_2 \omega_2 \qquad (6)$$

Here, T_1 is the torque produced by the internal combustion engine and ω_1 is its speed. Likewise, T_2 is the torque produced by the electric motor and ω_2 is its speed. If T_3 is the total torque ω_3 is the rotational speed of the wheels. Therefore, the torque coupler can be expressed as;

$$T_3 = T_1 k_1 + T_2 k_2 \qquad (7)$$

Here k_1 and k_2 are the structural parameters of the torque coupler and expressed as:

$$k_1 = \frac{\omega_1}{\omega_3} \; ; \; k_2 = \frac{\omega_2}{\omega_3} \qquad (8)$$

Again, k_1 and k_2 being the structural parameters of the speed coupler, the torque and speed expressions for the speed coupler are as follows in parallel with the torque coupler;

$$\omega_3 = k_1 \omega_1 + k_2 \omega_2 \qquad (9)$$

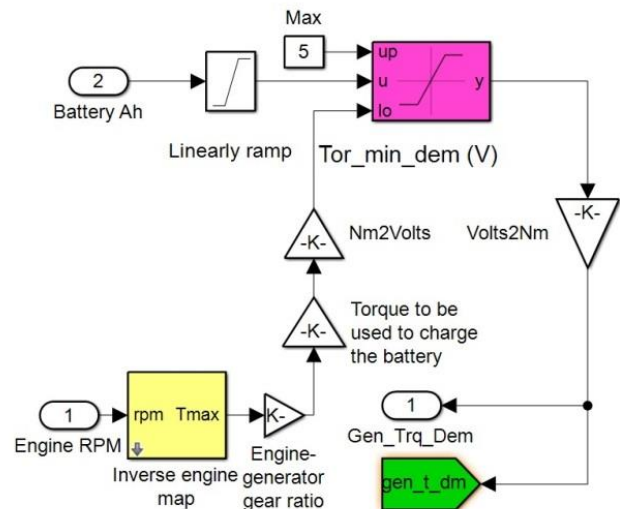$$T_3 = \frac{T_1}{k_1} + \frac{T_2}{k_2} \qquad (10)$$

Fig. 3.   Mode change model in hybrid electric vehicle(33)

3. Simulation

In this study, a parallel hybrid electric vehicle modeling was performed in Matlab/Simulink® environment. In the model presented in Figure 4, A 114 kW internal combustion engine and a 50 kW electric motor are used to provide hybrid electric vehicle power. In addition, batteries with four different chemistries, namely lithium iron phosphate, nickel metal hydride, nickel cadmium and lead acid were used in order to examine the effects of battery chemistries on the model. Each of the battery packs is configured as 350 Volt and 14 kWh.
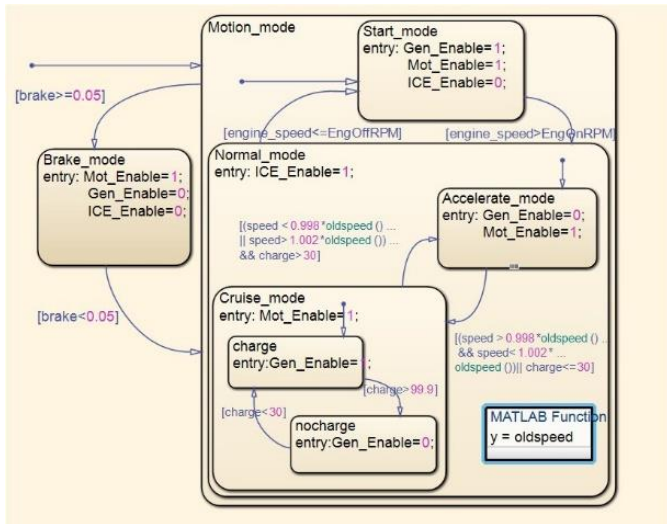
Fig. 4.   Generator working model

Hybrid mode term is used to activate the electric motor in cases where the power of the internal combustion engine is less efficient or to deactivate the electric motor when there is sufficient power. When the hybrid mode is active, the electric motor will be activated and the batteries will begin to discharge. When the hybrid mode is passive, the electric motor will be turned off and the batteries will start charging.
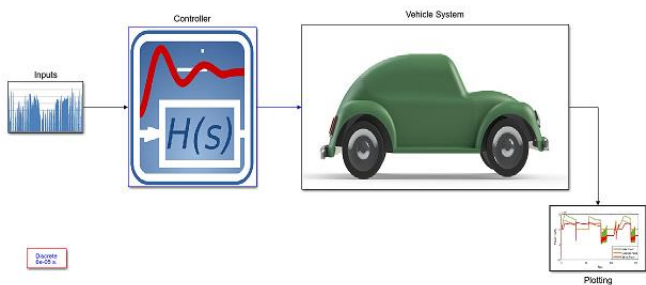

Fig. 5.   Hybrid electric vehicle model

The driving scenarios required for the hybrid electric vehicle model were created by using the black box data obtained from the trolleybusses operated by Malatya Municipality public transportation company (Motaş Inc). Accelerator pedal signals were used from the data and two different driving scenarios were cre-

ated. According to the data from Motaş Inc. two driving scenarios are formed. The first driving scenario is determined to be between 10.30 and 11.30 when passenger traffic is the slowest in the day. This scenario is presented in Fig 6.
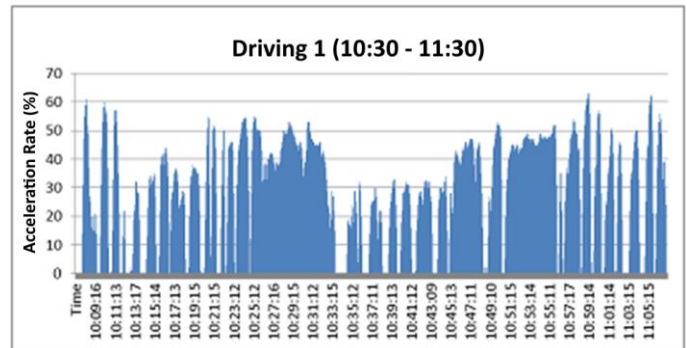

Fig. 6.   First driving scenario

The second driving scenario is set between 12.30 and 13.30, when the number of passengers are the most compared to the other times of the day. This signal is presented in Figure 7.
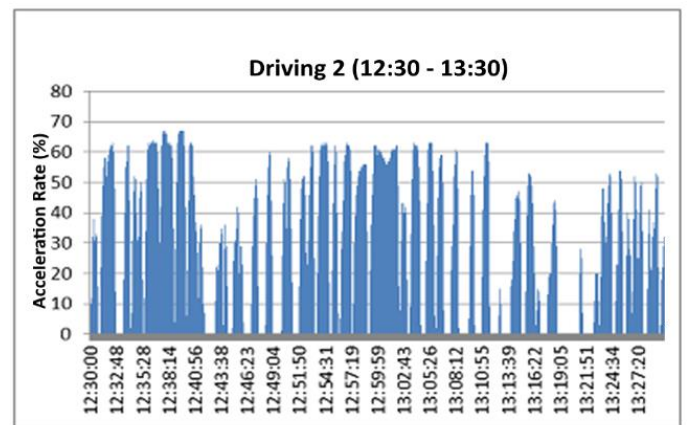

Fig. 7.   Second driving scenario

In the hybrid electric vehicle simulation, four different battery chemistries used on the vehicle and the discharge and charging power of the batteries analyzed for both driving scenarios. At the end of this trip, which was carried out during the heavy and light traffic conditions, the remaining state of charge (SoC) was examined and the most efficient battery type was analyzed.

4. Result and Discussions

The simulation has been prepared in Simulink® using MATLAB® 2020b software. The ideal sampling frequency of the simulation is 1 kHz. Ode23tb was used as solver. Each unit of time (T=1) in the simulation is equal to 23 seconds in real time. The simulation is ran for 60 minutes of real time. This time has been determined as T=156.52 in total on Matlab®. The simulation was made with the following assumptions:

- Switches and contacts are ideal.
- Batteries are completely healthy.

- Ambient temperature is constant 25 °C.

In the first driving scenario, the hybrid mode graph of the vehicle is presented in Figure 8. This mode change will be used for the four battery chemistries in the first driving scenario.
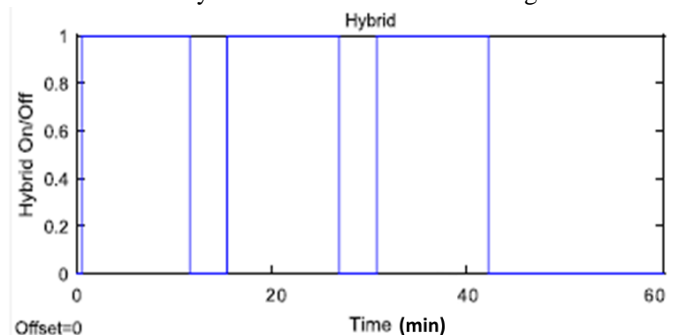

Fig. 8.   Hybrid mode switching during first driving scenario

Four different battery types were placed on the vehicle in the selected driving scenario and SoC analysis was performed with the determined battery powers. The battery, generator and engine power during the first driving scenario of the Lithium Iron Phosphate (LFP) battery are shown in Figure 9.
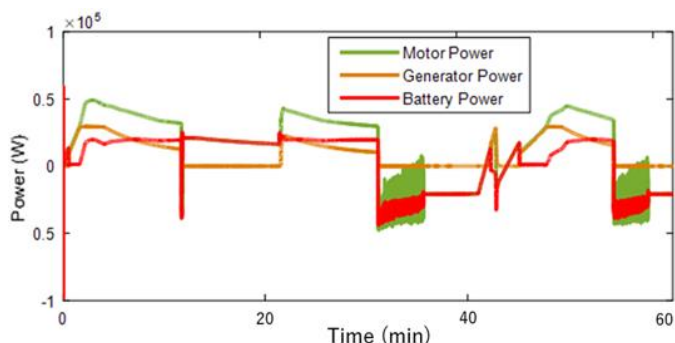

Fig. 9.   Power data when using LFP batteries

LFP battery was used to power 50 kW of electric motor until T=30 during the first driving scenario. Due to the high power requirement on the vehicle during the initial move, the electric motor worked at full capacity. Until this point, the hybrid mode was active as seen in Figure 8. The electric motor was deactivated until T=40 and only the internal combustion engine was effective to drive the vehicle. Between T=55 and T=80, the electric motor was activated again and continued to operate with 50 kW full load. When the hybrid mode is off, the electric motor is deactivated, and when the hybrid mode is on, the electric motor is activated. As soon as the electric motor is active, the batteries will be discharged and the batteries will be charged when the hybrid mode is off. Battery charging is provided by the generator placed on the hybrid electric vehicle model. As soon as the electric motor is deactivated, the generator will start and charge the batteries with a maximum power of 30 kW. This situation will also affect the SoC of the LFP battery. The SoC change of this battery type during the trip is shown in Figure 10.
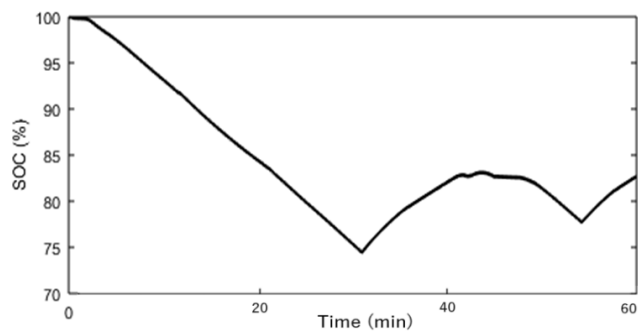

Fig. 10.   SoC status of LFP batteries

The test was started with the SoC value of 100% for the LFP battery and the SoC status was 82% at the end of the run. The battery, generator and engine power during the first driving scenario of the Nickel Metal Hydride (Ni-MH) battery are shown in Figure 11.
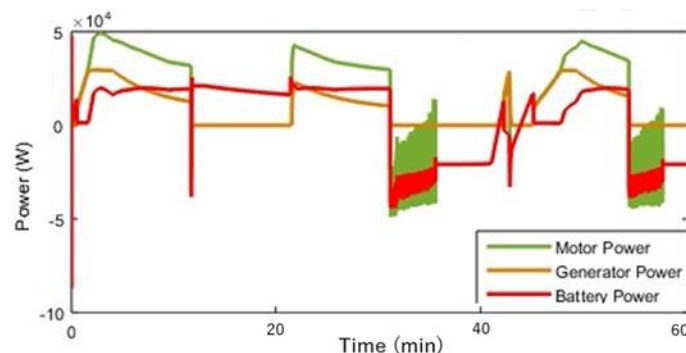

Fig. 11.   Power data using Ni-MH batteries

During the first driving scenario, the Ni-MH battery began to be discharged at first. With the hybrid mode on, the electric motor was activated at T=0 and T=30 instantly and the vehicle started driving with a power of 50 kW. Since hybrid changes occur at three different instances, the electric motor has also been activated at three different instances. This situation had an effect on the charge and discharge of the Ni-MH battery. The SoC graph that occurs during the trip is given in figure 12.
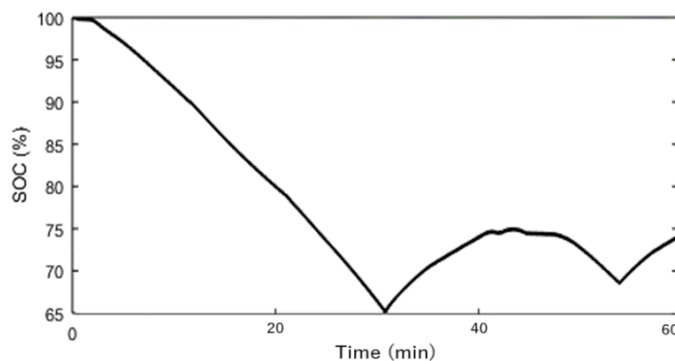

Fig. 12.   SoC status of Ni-MH batteries

The simulation was started with 100% SoC and this value at the end of the run was 74%. In this driving mode, the charge capacity of Ni-MH batteries has decreased by 26%. Lead Acid battery is the third type of battery used for this driving mode. The battery, generator and engine power generated during driving are shown in Figure 13.
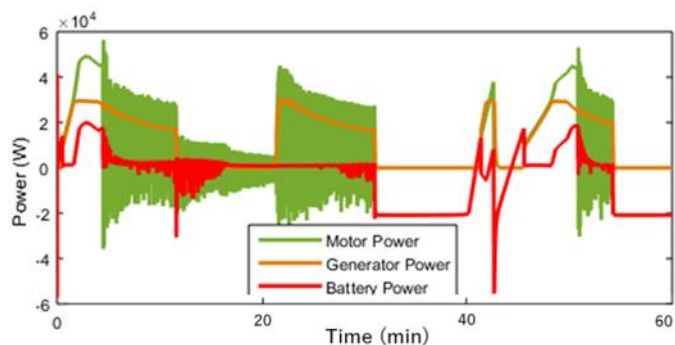

Fig. 13.   Power data using lead-acid batteries

Between T=0 and T=55, the electric motor supported the driving with a supplied power of 55 kW. Later, the power of the electric motor decreased over time and it was completely deactivated at T=55. Between T=55 and T=100, the electric motor was not active. Afterwards, it starts working in conjunction with the internal combustion engine. At the end of the simulation, the SoC status of the Lead-Acid battery is given in Figure 14.
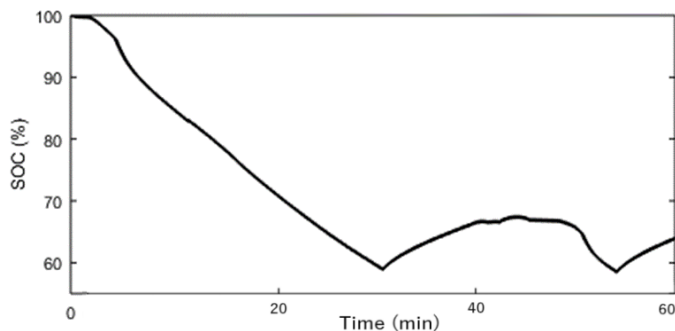

Fig. 14.   SoC status of lead-acid batteries

The Lead-Acid battery was used within the first driving scenario with a 100% SoC, and at the end of the simulation, the SoC was calculated as 64%. There was a total loss of 36% during the drive. At this stage, the lead acid battery has been further discharged. Finally, Nickel Cadmium (Ni-Cd) battery type was used with the first driving scenario. The battery, generator and engine power generated during driving are shown in Figure 15.
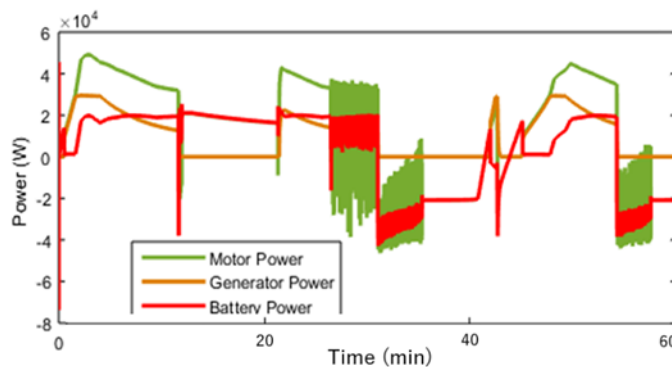

Fig. 15.   Power data using ni-cd batteries

Here, it was observed that the electric motor was activated at three instances. The electric motor included in the system with a power of 55 kW, causing the batteries to be discharged. The electric motor, which was switched on for the third time between T=110 and T=140, was not activated until the end of the simulation. The SoC graph of the battery after a one hour simulation is given in Figure 16.
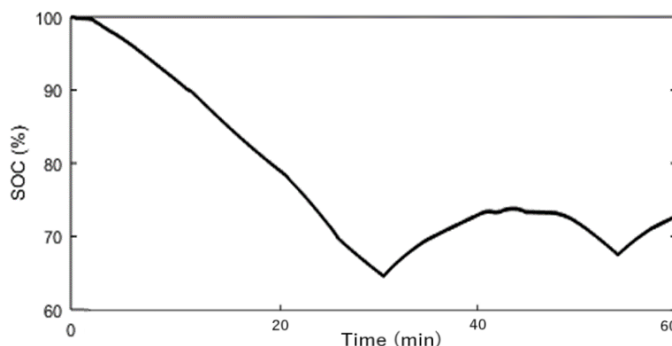

Fig. 16.   SoC status of Ni-Cd batteries

At the end of the first driving scenario, the charge and discharge characteristics of the batteries according to the hybrid mode are examined. The first factor in the charging and discharging of the batteries is the hybrid mode, and as the hybrid mode is activated the electric motor charges or discharges the batteries. Nickel Cadmium battery has a 72% SoC at the end of the simulation. The second driving mode, on the other hand, was made with the data gathered between 12:30 and 13:30, which is the busiest time of the day, as shown in Figure 7.
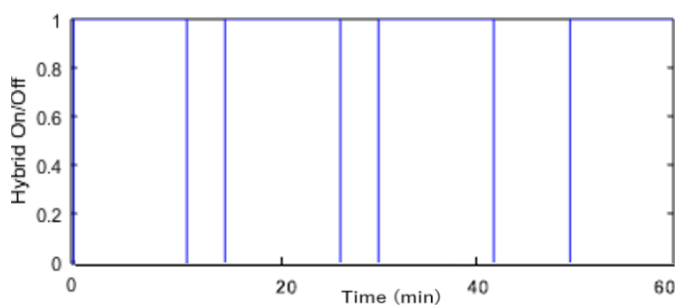

Fig. 17.   Hybrid mode switching during second driving scenario

More hybrid mode changes observed on the hybrid vehicle at these time intervals. Frequent full stops and accelerations increase the need for the electric drive in this scenario. The hybrid mode change that occurred in the vehicle during this time period is shown in Figure 17.
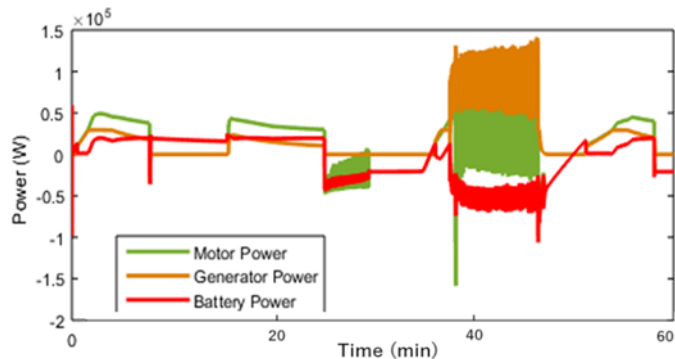

Fig. 18.   Power data when using LFP batteries

In total, hybrid mode changes occurred at four instances. At these instances, the electric motor was enabled to be switched on and off.

In the second driving scenario, LFP battery was used first. The battery, generator and engine power during the trip are shown in Figure 18.

When the above data are examined, hybrid mode changes occurred between T=0 and T=20, between T=40 and T=60, between T=100 and T=120, and finally between T=130 and T=145. In the first three changes, the electric motor producing a total of 50 kW of power was activated, and this power was measured as 55 kW. The SoC during the simulation is given in Figure 19.
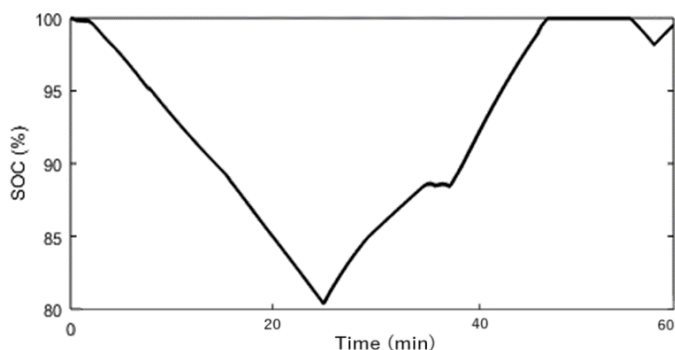

Fig. 19.   SOC status of LFP batteries

When the SoC graph was examined, it was seen that the lithium iron phosphate battery that started in full charge following a 20% decrease and then increased to 100% back again. The battery, which was slightly discharged in the last hybrid mode change, went down to 97% and recharged to 100% again. The second type of battery used with the second driving scenario is Nickel Metal Hydride. The battery power, generator and engine generated during driving are shown in Figure 20.
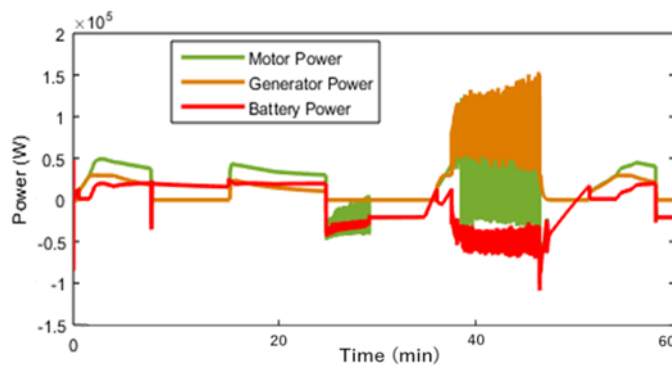

Fig. 20.   Power data using Ni-MH batteries

When the graph was examined, it was seen that the hybrid mode was on at four different instances where the batteries were discharged. In the first three hybrid mode changes, the electric motor was operated with 50 kW and in the last mode change it was operated with 55 kW. The SoC status of the batteries during one hour drive is given in Figure 21.
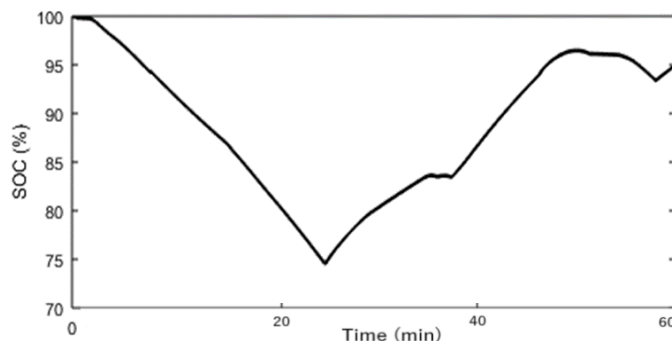
Fig. 21.   SoC status of Ni-MH batteries

Ni-MH battery has been discharged to 75%. The SoC could not reach 100% until the end of simulation. It completed the simulation with 95% SoC. The third type of battery used with the second driving scenario is Lead acid. The battery, generator and engine power generated during driving are shown in Figure 22.
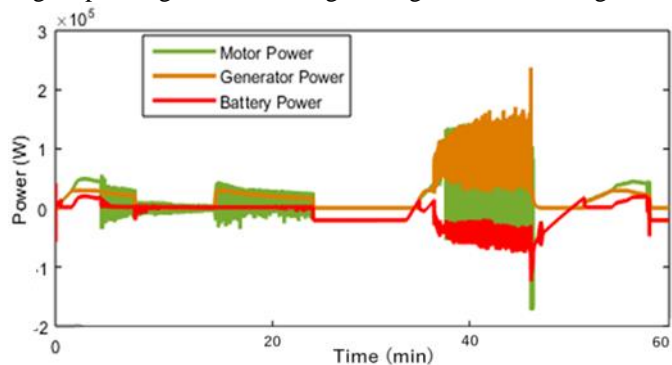
Fig. 22.   Power data using Lead-Acid batteries

Like the other two batteries, the Ni-MH battery has experienced a total of four hybrid mode changes. In the last hybrid

mode change, it provided additional power to the internal combustion engine with a power of 55 kW. The SoC chart formed during the simulation is presented in Figure 23.

Fig. 23.   SoC status of Lead-Acid batteries

Lead-Acid was discharged to 65% SoC during simulation. Next, the battery simulation started charging the batteries and the simulation was completed with a charge rate of 83%. It has less SoC at the end of the simulation compared to the other two battery types. The last battery type used with the second driving scenario is Nickel-Cadmium. The battery, generator and engine power generated during driving are shown in Figure 24.

Fig. 24.   Power data using Ni-Cd batteries

When examined, it was seen that there were hybrid mode changes at four different instances depending on the hybrid mode change. The SoC chart formed during the trip is presented in Figure 25.
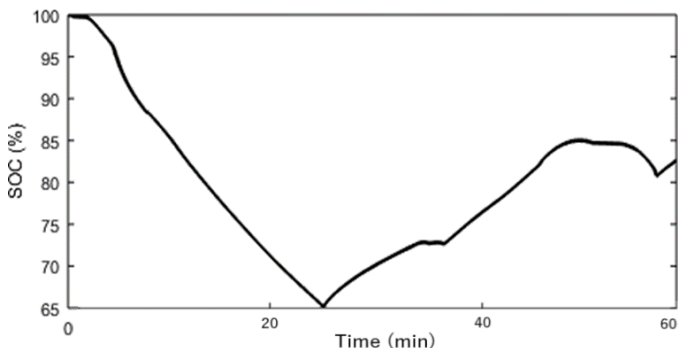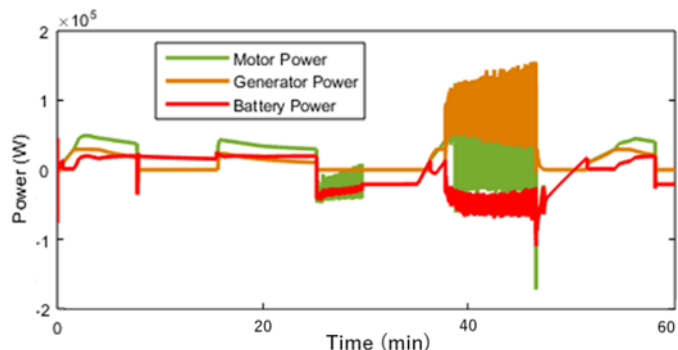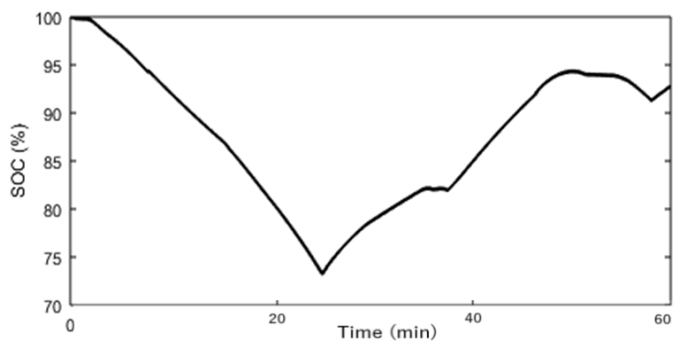

Fig. 25. SoC status of Ni-Cd batteries

The Ni-Cd battery was discharged up to 74% SoC during the simulation. When the simulation was terminated, the state of charge was measured as 92.5%. This state of charge rate shows that nickel cadmium battery is more efficient than lead acid battery. However, when compared to Nickel Metal Hydride and Lithium Iron Phosphate batteries, Ni-Cd is observed to be less efficient.

5. Conclusion

In this study, battery modeling of a hybrid electric vehicle with four different chemistries was performed and realistic results were obtained by applying the black box data obtained from public transportation on the hybrid model. In the first driving scenario, the electric motor is positioned to support the internal combustion engine reaching the highest power level of 50 kW with the hybrid mode is on. In addition, when the hybrid mode is off, the generator has been activated with a power of 30 kW, allowing all batteries to be charged.

During the charge and discharge changes in hybrid mode, battery capacity readings are fluctuated. This is because when the battery starts charging, the voltage instantly increase followed by slow increase in voltage until it becomes stable at fully charged. Similarly, opposite case is true for the discharging case. In the first driving scenario, the initial conditions were taken as 100% SoC and it was observed that the battery with the highest SoC value at the end of the simulation was LFP. The lithium iron phosphate battery was found to be the most efficient battery type in these test criteria. In addition, the lead acid was observed to be the most inefficient battery type with 64% SoC value at the end of the simulation under these test conditions. SoC values of the batteries at the end of the simulations are given in Table 2.

Table 2. SoC values of the batteries at the end of the test according to the first driving scenario

	Initial SoC	Minimum SoC	Final SoC
LFP	100%	%78	82%
Nickel Metal Hydrate	100%	%72	76%
Lead Acid	100%	%59	64%
Nickel Cadmium	100%	%66	72%

In the second driving scenario, the initial conditions of all batteries were selected as 100% SoC. In the test that is conducted during the busiest hours of the day, the battery type that reached the lowest SoC value was Lead Acid. At the end of the simulation, the battery type with the highest capacity was Lithium iron phosphate. According to the parameters of the second driving scenario, the most efficient battery type was LFP and the most inefficient battery type was lead acid. The SoC values of the batteries at the end of the simulations are given in Table 3.

Table 3. Soc values of the batteries at the end of the test according to the second driving scenario

	Initial SoC	Minimum SoC	Final SoC
LFP	100%	80%	100%
Nickel Metal Hydrate	100%	75%	95%
Lead Acid	100%	65%	83%
Nickel Cadmium	100%	74%	93%

As a result of the study, efficiency analysis of the batteries with four different battery chemistries used in a hybrid electric vehicle model was performed for two different driving scenarios. According to these analysis, lithium iron phosphate batteries have been determined as the most ideal battery type for hybrid electric vehicles. On the contrary, lead acid batteries found to be the most inefficient battery type.

Table 4. Cost of batteries by type for the 14 kwh battery capacity used on the hybrid electric car model (34)

Battery Types	kWh Price (2020)	Total Price
LFP	137 $	1918 $
Nickel Metal Hydrate	300 $	4200 $
Lead Acid	200 $	2800 $
Nickel Cadmium	350 $	4900 $

Considering the SoC ratio, it has been observed that compared to the other battery types, a lithium iron phosphate battery can extend the driving range for a hybrid electric vehicle under the same conditions. The battery type providing the shortest range was lead acid. The order of the batteries from the longest range to the shortest range is respectively: Lithium iron phosphate, nickel metal hydride, nickel cadmium and lead acid. Cost analysis of the 14 kWh battery capacity used on the hybrid electric car model is shown in Table 4.

According to the table, the most economical battery type is lithium iron phosphate with total cost of 1918 dollars. Constructing a battery pack with lead acid batteries costs 2800 dollars. The most expensive battery chemistry that can be used on the vehicle is Nickel Cadmium. In order to create 14 kWh battery capacity, in total 4900 dollars must be spent. In future studies, this subject can be examined in detail with new driving scenarios and new types of vehicle models.

Acknowledgment

Conflict of Interest Statement

The authors declare that there is no conflict of interest in the study.

CRediT Author Statement

Yunus Emre Ekici: Conceptualization, Methodology, Software, Writing-original draft, Visualization,

İsmail Can Dikmen: Writing-original draft, translation and methodology,

Mustafa Nurmuhammed: Writing-original draft, translation and methodology,

Teoman Karadağ: Supervision,

References

[1] Anseán D, González M, García VM, Viera JC, Antón JC, Blanco C. Evaluation of LiFePO4 Batteries for Electric Vehicle Applications. IEEE Trans Ind Appl. 2015;51(2):1855–63.

[2] Khaligh A, Li Z. Battery, ultracapacitor, fuel cell, and hybrid energy storage systems for electric, hybrid electric, fuel cell, and plug-in hybrid electric vehicles: State of the art. IEEE Trans Veh Technol. 2010;59(6):2806–14.

[3] Oncken J, Chen B. Real-Time Model Predictive Powertrain Control for a Connected Plug-In Hybrid Electric Vehicle. IEEE Trans Veh Technol. 2020;69(8):8420–32.

[4] Chen X, Shen W, Vo TT, Cao Z, Kapoor A. An overview of lithium-ion batteries for electric vehicles. 10th Int Power Energy Conf IPEC 2012. 2012;230–5.

[5] Scrosati B, Garche J. Lithium batteries: Status, prospects and future. J Power Sources. 2010;195(9):2419–30.

[6] Amrhein M, Krein PT. Dynamic simulation for analysis of hybrid electric vehicle system and subsystem interactions, including power electronics. IEEE Trans Veh Technol. 2005;54(3):825–36.

[7] Ducusin M, Gargies S, Mi C. Modeling of a series hybrid electric high-mobility multipurpose wheeled vehicle. IEEE Trans Veh Technol. 2007;56(2):557–65.

[8] Ghorbani R, Bibeau E, Filizadeh S. On conversion of hybrid electric vehicles to plug-in. IEEE Trans Veh Technol. 2010;59(4):2016–20.

[9] Tyrus JM, Long RM, Kramskaya M, Fertman Y, Emadi A. Hybrid electric sport utility vehicles. IEEE Trans Veh Technol. 2004;53(5):1607–22.

[10] He X, Maxwell T, Parten ME. Development of a hybrid electric vehicle with a hydrogen-fueled IC engine. IEEE Trans Veh Technol. 2006;55(6):1693–703.

[11] Raghavan SS, Khaligh A. Electrification potential factor: Energy-based value proposition analysis of plug-in hybrid electric vehicles. IEEE Trans Veh Technol. 2012;61(3):1052–9.

[12] Emadi A, Rajashekara K, Williamson SS, Lukic SM. Topological overview of hybrid electric and fuel cell vehicular power system architectures and configurations. IEEE Trans Veh Technol. 2005;54(3):763–70.

[13] Ho JC, Huang YHS. Evaluation of electric vehicle power technologies. PICMET 2014 - Portl Int Cent Manag Eng Technol Proc Infrastruct Serv Integr. 2014;2843–7.

[14] Zhao C, Zu B, Xu Y, Wang Z, Zhou J, Liu L. Design and analysis of an engine-start control strategy for a single-shaft parallel hybrid electric vehicle. Energy. 2020;202(5):2354–63.

[15] Ceraolo M, di Donato A, Franceschi G. A general approach to

energy optimization of hybrid electric vehicles. IEEE Trans Veh Technol. 2008;57(3):1433–41.

[16] Filippa M, Mi C, Shen J, Stevenson RC. Modeling of a hybrid electric vehicle powertrain test cell using bond graphs. IEEE Trans Veh Technol. 2005;54(3):837–45.

[17] Moons I, de Pelsmacker P. Emotions as determinants of electric car usage intention. J Mark Manag. 2012;28(3–4):195–237.

[18] How DNT, Hannan MA, Hossain Lipu MS, Ker PJ. State of Charge Estimation for Lithium-Ion Batteries Using Model-Based and Data-Driven Methods: A Review. IEEE Access. 2019;7:136116–36.

[19] Pohl H, Elmquist M. Radical innovation in a small firm: A hybrid electric vehicle development project at Volvo Cars. R D Manag. 2010;40(4):372–82.

[20] Ferdowsi M. Plug-in hybrid vehicles - A vision for the future. VPPC 2007 - Proc 2007 IEEE Veh Power Propuls Conf. 2007;457–62.

[21] Zhu ZQ, Cai S. Hybrid excited permanent magnet machines for electric and hybrid electric vehicles. CES Trans Electr Mach Syst. 2019;3(3):233–47.

[22] Chan CC, Bouscayrol A, Chen K. Electric, hybrid, and fuel-cell vehicles: Architectures and modeling. IEEE Trans Veh Technol. 2010;59(2):589–98.

[23] Albert IJ, Member S, Kahrimanovic E, Emadi A, Member S. Hybrid Electric Drive Trains. 2004;53(4):1247–56.

[24] Song Z, Liu C, Zhao H. Investigation on Magnetic Force of a Flux-Modulated Double-Rotor Permanent Magnet Synchronous Machine for Hybrid Electric Vehicle. IEEE Trans Transp Electrif. 2019;5(4):1383–94.

[25] Xu B, Hu X, Tang X, Lin X, Li H, Rathod D, et al. Ensemble Reinforcement Learning-Based Supervisory Control of Hybrid Electric Vehicle for Fuel Economy Improvement. IEEE Trans Transp Electrif. 2020;6(2):717–27.

[26] Dikmen İC, Ekici YE, Karadağ T, Abbasov T, Hamamci SE. Electrification in Urban Transport: A Case Study with Real-time Data. Balk J Electr Comput Eng. 2021;9(1):69–77.

[27] Ekici YE, Tan N. Farklı Batarya Tiplerinin Şarj ve Deşarj Karakteristiklerinin Hibrit Araç Modeli Üzerinde İncelenmesi. In: International Conferance on Innovatiive Engineering Applications. Sivas; 2018. p. 848–55.

[28] Zhang WJ. Structure and performance of LiFePO4 cathode materials: A review. J Power Sources [Internet]. 2011;196(6):2962–70. Available from: http://dx.doi.org/10.1016/j.jpowsour.2010.11.113

[29] Xiaodong Q, Qingnian W, YuanBin Y. Power demand analysis and performance estimation for active-combination energy storage system used in hybrid electric vehicles. IEEE Trans Veh Technol. 2014;63(7):3128–36.

[30] Deepankar E, Chauhan AK, Singh SK. Integrated Dual-Output L-Z Source Inverter for Hybrid Electric Vehicle. IEEE Trans Transp Electrif. 2018;4(3):732–43.

[31] Gong Q, Li Y, Peng ZR. Trip-based optimal power management of plug-in hybrid electric vehicles. IEEE Trans Veh Technol. 2008;57(6):3393–401.

[32] Su Y, Su L, Hu M, Qin D, Fu C, Yu H. Modeling and Dynamic Response Analysis of a Compound Power-Split Hybrid Electric Vehicle During the Engine Starting Process. IEEE Access. 2020;8:186585–98.

[33] Ekici YE. Batarya Yönetim Sistemleri. Yüksek Lisans Tez. İnönü Üniversitesi. 2019.

[34] BloombergNEF. Battery Pack Prices Cited Below $100/kWh for the First Time in 2020, While Market Average Sits at $137/kWh [Internet]. 2020. Available from: https://about.bnef.com/blog/battery-pack-prices-cited-below-100-kwh-for-the-first-time-in-2020-while-market-average-sits-at-137-kwh/